Anomalous diffusion in confined turbulent convection

G. Boffetta,[1] F. De Lillo,[1] and S. Musacchio[2]

[1]*Dipartimento di Fisica and INFN, Università di Torino, via Pietro Giuria 1, 10125 Torino, Italy*
[2]*CNRS UMR 7351, Laboratoire J.A. Dieudonné, Université de Nice Sophia Antipolis, Parc Valrose, 06108 Nice, France*

Turbulent convection in quasi-one-dimensional geometry is studied by means of high-resolution direct numerical simulations within the framework of Rayleigh-Taylor turbulence. Geometrical confinement has dramatic effects on the dynamics of the turbulent flow, inducing a transition from superdiffusive to subdiffusive evolution of the mixing layer and arresting the growth of kinetic energy. A nonlinear diffusion model is shown to reproduce accurately the above phenomenology. The model is used to predict, without free parameters, the spatiotemporal evolution of the heat flux profile and the dependence of the Nusselt number on the Rayleigh number.

I. INTRODUCTION

Diffusion in systems of reduced dimensionality displays a number of peculiarities in comparison with the unconfined three-dimensional (3D) space. This feature has been studied in simple systems in which geometrical confinement leads to subdiffusive behavior of trajectories [1,2]. In the present paper we study, by means of high-resolution numerical simulations, the effects of confinement in quasi-1D geometry on turbulent convection within the framework of Rayleigh-Taylor (RT) turbulence. RT turbulence is a prototypical example of turbulent convection which arises from the instability at the interface of two layers of fluids at different densities in a gravitational field [3]. It is relevant for several problems in natural and applied sciences, like cloud formation [4], the physics of supernovae [5], and inertial confinement fusion [6].

In three dimensions, RT instability evolves in a turbulent mixing layer whose width grows proportionally to gt^2 in the direction of gravity g [5,7]. Inside the mixing layer, the conversion of potential energy to kinetic energy sustains a turbulent cascade characterized by Kolmogorov-Obukhov phenomenology for velocity and temperature fluctuations [5,8–12]. The integral scale of the turbulent flow follows the accelerated growth of the width of the mixing layer. Because of the absence of thermal and kinetic boundary layers, the time dependence of Rayleigh, Reynolds, and Nusselt numbers in RT turbulence realizes the Kraichnan scaling regime associated with the ultimate state of thermal convection [13,14].

In the following we show that the confinement of the flow in the two directions normal to the acceleration of gravity has dramatic effects on the dynamics of the flow as it modifies the late stage evolution of the mixing layer from t^2 to a subdiffusive law and changes qualitatively the evolution of other large scale quantities, such as kinetic energy. In order to understand the observed phenomenology, we propose a simple nonlinear diffusion model, based on Prandtl's mixing length theory, which reproduces the behavior of the mixing layer and accurately predicts the shape of mean temperature and heat flux profiles. The diffusion model also predicts, without free parameters, the dependence of Nusselt and Reynolds numbers on the Rayleigh number of the flow, showing the effect of confinements on the ultimate state of thermal convection, in agreement with numerical results.

II. RAYLEIGH-TAYLOR TURBULENCE IN QUASI-1D GEOMETRY

The equation of motion for the incompressible velocity field $\mathbf{v}$ ($\nabla \cdot \mathbf{v} = 0$) and temperature field T in the Boussinesq approximation is

$$\partial_t \mathbf{v} + \mathbf{v} \cdot \nabla \mathbf{v} = -\nabla p + \nu \nabla^2 \mathbf{v} - \beta \mathbf{g} T, \qquad (1)$$

$$\partial_t T + \mathbf{v} \cdot \nabla T = \kappa \nabla^2 T, \qquad (2)$$

where β is the thermal expansion coefficient, ν is the kinematic viscosity, κ is the thermal diffusivity, and $\mathbf{g} = (0,0,-g)$ is the gravitational acceleration.

We will consider a quasi-one-dimensional setup in which the flow is confined in a box of dimensions $L_z \gg L_x = L_y$. The initial condition (at $t = 0$) is a layer of cooler (heavier) fluid on the top of a hotter (lighter) layer at rest, i.e., $\mathbf{v}(\mathbf{x},0) = 0$ and $T(\mathbf{x},0) = -(\theta_0/2)\mathrm{sgn}(z)$, where θ_0 is the initial temperature jump ($T = 0$ is the reference mean temperature). This initial configuration is unstable, and after the initial linear phase, the system develops a turbulent mixing layer which grows in time starting from the plane $z = 0$ (see an example in Fig. 1).

We have simulated Eqs. (1) and (2) in a domain of size $L_x = L_y = \pi/4$, $L_z = 8\pi$ at resolutions up to $N_x = N_y = 256$, $N_z = 8192$ with a fully dealiased parallel pseudospectral code with periodic boundary conditions. Parameters are $\theta_0 = 1.0$, $\beta g = 0.5$, and $\nu = \kappa = 10^{-4}$. In all the results, the time is expressed in terms of the characteristic transverse time $\tau = (L_x/\beta g \theta_0)^{1/2}$. We remark that the confinement in the present simulations is not obtained by imposing physical boundaries on lateral sides but only by imposing periodicity on a scale $L_x = L_y \ll L_z$. Nonetheless, we found that the evolution of the mixing layer is similar to that observed in experiments with physical boundaries on the lateral sides. This indicates that the suppression of modes at scales larger than L_x is sufficient to induce the quasi-1D behavior and that large scale properties of the flow are apparently independent of the lateral boundary conditions.

The initial unstable condition for the temperature field $T(\mathbf{x},0) = -(\theta_0/2)\mathrm{sgn}(z)$ is numerically smoothed with a tanh function over a few grid points. Moreover, in order to trigger the instability, the interface is "diffused" around $z = 0$ by
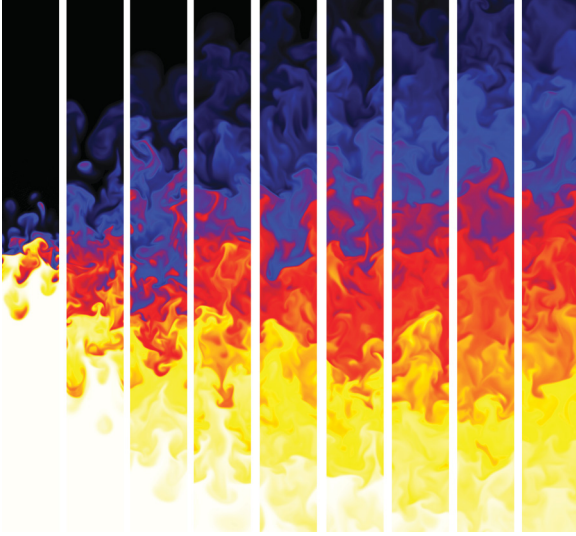
FIG. 1. (Color online) Vertical sections of the temperature field T in the central part of the computational domain equispaced in time with $\Delta t = 8\tau$ (from left to right). White represents hot temperatures $\theta_0/2$, and black represents cold temperatures $-\theta_0/2$.

adding a small amplitude of white noise to the temperature field in the smoothing region.

In the fully three-dimensional case, after the first instability the growth of the mixing layer width h is known to follow a quadratic law $h(t) \simeq \beta g \theta_0 t^2$ [5,10,12] as a consequence of constant acceleration. In the present setup, we indeed observe an initial stage of accelerated growth, but because of the lateral confinement, the time evolution of the mixing layer at times much larger than the typical transverse time scale $\tau = (L_x/\beta g \theta_0)^{1/2}$ becomes slower than linear as shown in Fig. 1 and more quantitatively in Fig. 2.

Another, and related, important effect of the confinement concerns the energy balance. In the mixing layer turbulent
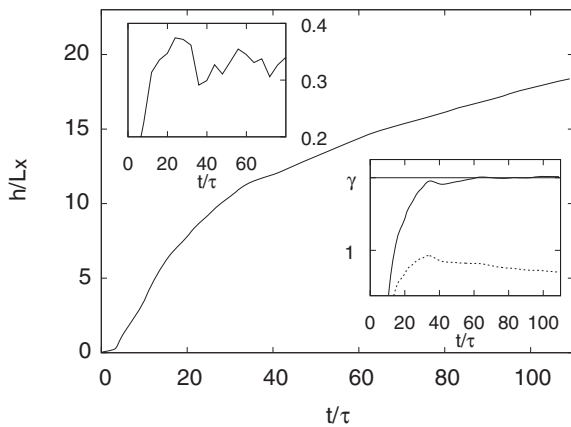

FIG. 2. Time evolution of the mixing layer width $h(t)$ obtained from the fit of $z_1(t)$ according to Eq. (7). Lower inset: $h(t)$ compensated with the behavior predicted by the nonlinear diffusion model $2(\beta g \theta_0)^{1/5} L_x^{4/5} t^{2/5}$ (continuous line), giving the value of the coefficient $\gamma = 1.40 \pm 0.02$ together with the compensation with diffusive behavior $t^{1/2}$ (dotted line). Upper inset: Velocity correlation scale $\mathcal{L}$, normalized with L_x as a function of time.
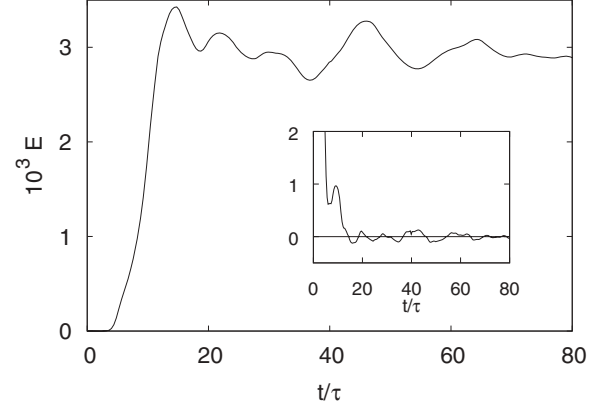

FIG. 3. Total kinetic energy E compensated with the rms velocity $u_{rms} = \beta g \theta_0 L_x$ as a function of time. Inset: Ratio of dE/dt to viscous energy dissipation ε_ν.

kinetic energy $E = (1/2)\langle v^2 \rangle$ is produced at the expense of potential energy $P = -\beta g \langle zT \rangle$ as the energy balance indicates

$$-\frac{dP}{dt} = \beta g \langle wT \rangle = \frac{dE}{dt} + \varepsilon_\nu, \qquad (3)$$

where $\varepsilon_\nu = \nu \langle (\partial_\alpha v_\beta)^2 \rangle$ is the viscous energy dissipation, $\langle \rangle$ represents the integral over the physical domain, and we have neglected the effects of molecular diffusivity on potential energy. Indeed, the contribution of the molecular diffusivity $\kappa \beta g \theta_0 L_x^2$ to the dissipation rate of the potential energy is negligible with respect to the contribution of the advective term $\beta g \langle wT \rangle$. Their ratio is given by the Nusselt number $Nu = \langle wT \rangle/(\kappa \theta_0 L_x^2)$, which is much larger than unity in the turbulent stage of the evolution. In three-dimensional RT convection it is known that all the terms in Eq. (3) scale in the same way, and one has $dE/dt \simeq \varepsilon_\nu \simeq (1/2)\beta g \langle wT \rangle$ [15]. Physically, this means that the integral scale follows $h(t)$, and consistently large scale velocity fluctuations (which generate the turbulent cascade with flux ε_ν) grow linearly in time $u_{rms} \simeq \beta g \theta_0 t$. In the present configuration, when the mixing layer growth enters in the slow, one-dimensional regime at $t \gtrsim 30\tau$, turbulent kinetic energy saturates as shown in Fig. 3, and viscous dissipation becomes dominant in the balance of Eq. (3).

The confinement affects also the typical size of the thermal plumes. The horizontal size of thermal plumes is clearly bounded by the confining scale L_x. On the contrary, the flow has no geometrical constraint in the vertical direction. This could *a priori* allow for the development of narrow plumes longer than L_x. Nevertheless, the temperature fields obtained in our simulations do not display such strongly elongated structures (see e.g., Fig. 1). To investigate this issue, we measured the correlation function $C(r) = \langle v_z(\mathbf{x} + \mathbf{r}) v_z(\mathbf{x}) \rangle/\langle v_z^2 \rangle$ of the vertical velocity v_z in the vertical direction $\mathbf{r} = (0, 0, r)$. An estimate of the characteristic length of plumes is provided by the the vertical velocity correlation scale $\mathcal{L}$, here defined as the width at half-height of the correlation function $C(\mathcal{L}) = 1/2 C(0)$. In the first stage of the evolution, the correlation scale $\mathcal{L}$ grows following the evolution of the width of the mixing layer. When the one-dimensional regime sets in (at $t \gtrsim 30\tau$), the velocity correlation scale $\mathcal{L}$ saturates to a value $\sim L_x$ (see the inset of Fig. 2). A similar behavior is

observed for the correlation scale in the vertical direction of the horizontal components of the velocity (not shown). These findings indicate that the typical length of thermal plumes does not exceed the confining scale L_x. The absence of long narrow plumes is caused by the turbulent mixing which develops at scales smaller than L_x. It efficiently decorrelates the flow also in the vertical direction preventing the formation of strongly elongated structures. It is worthwhile to notice that such a mechanism may not be effective in the case of convective flows at high Prandtl number $Pr = \nu/\kappa$ in which turbulence is suppressed by the strong viscosity, and the presence of a long narrow plume cannot be excluded.

III. MODELING THE GROWTH OF THE MIXING LAYER

The independence of velocity fluctuations at scales larger than $\mathcal{L}$ allows to introduce an eddy diffusivity model for the vertical temperature profile which reproduces the one-dimensional regime of the evolution observed in the simulations.

The evolution equation for the vertical temperature profile $\overline{T}(z,t)$ is obtained by averaging Eq. (2) over L_x and L_y:

$$\partial_t \overline{T} + \partial_z \overline{wT} = \kappa \partial_z^2 \overline{T}, \qquad (4)$$

where w represents the vertical velocity. The thermal flux term $\overline{wT}$ makes Eq. (5) not closed. We close this equation in terms of an eddy diffusivity $K(z,t)$ so that Eq. (4) is rewritten as

$$\partial_t \overline{T} = \partial_z K(z,t) \partial_z \overline{T}. \qquad (5)$$

The eddy diffusivity is given dimensionally by $K \simeq u_{\text{rms}} \mathcal{L}$, and the typical velocity fluctuation can be estimated by balancing inertial and buoyancy terms in Eq. (1) as $u_{\text{rms}}^2/\mathcal{L} \simeq \beta g \theta_{\mathcal{L}}$, where $\theta_{\mathcal{L}}$ is the temperature difference across the scale $\mathcal{L}$ which forces u_{rms}. When $h(t) < L_x, \theta_{\mathcal{L}} = \theta_0$, and the diffusion model has been used to predict the shape of the temperature profile in the accelerated three-dimensional regime [14]. On the contrary, when $h(t) > L_x$, the integral scale saturates at $\mathcal{L} \simeq L_x$, and one estimates $\theta_{\mathcal{L}} \simeq L_x \partial_z \overline{T}$. Therefore, Eq. (5) becomes

$$\partial_t \overline{T} = a(\beta g)^{1/2} L_x^2 \partial_z (\partial_z \overline{T})^{3/2}, \qquad (6)$$

where a is a dimensionless coefficient which cannot be determined by dimensional arguments. A simple power counting in Eq. (6) gives for the growth of the mixing layer in this quasiunidimensional regime a subdiffusive behavior [16] $h(t) \simeq (\beta g \theta_0)^{1/5} L_x^{4/5} t^{2/5}$ in agreement with previous predictions and measurements [17,18].

Model (6) belongs to a class of nonlinear diffusion equations for which the self-similar solution starting from the step initial condition is known and for the present case reads [19–21]

$$\overline{T}(z,t) = -\theta_0 \frac{15}{16} \left[\frac{1}{5} \left(\frac{z}{z_1} \right)^5 - \frac{2}{3} \left(\frac{z}{z_1} \right)^3 + \frac{z}{z_1} \right] \qquad (7)$$

for $|z| \leqslant z_1$ and $\overline{T}(z) = \pm \theta_0/2$ for $|z| > z_1$. The half-width of the mixing layer grows as $z_1(t) = \gamma (\beta g \theta_0)^{1/5} L_x^{4/5} t^{2/5}$ with $\gamma = (a^2 15^3/16)^{1/5}$.

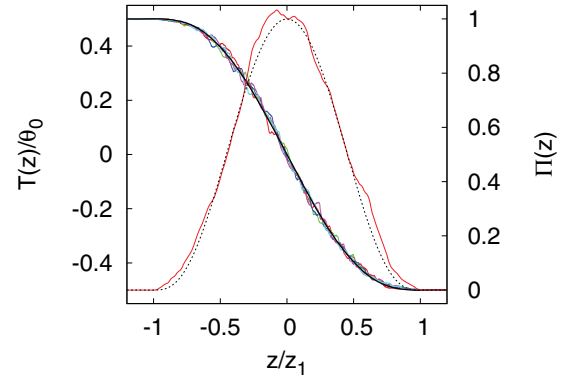Figure 4 shows that Eq. (7) provides a good fit of the temperature profiles obtained from numerical simulations.

FIG. 4. (Color online) Mean temperature profiles $\bar{T}(z,t)$ as a function of the rescaled variable z/z_1 at times $t/\tau = 70, 80, 90, 100, 110$ together with the theoretical prediction (7) (solid, smooth black line) which is used to fit the values of $z_1(t)$. Left y axis: Heat flux $\overline{wT}$ (red, continuous line) compensated with $\gamma^{5/2} \theta_0 L_x^2 (\beta g \theta_0)^{1/2}/(16 z_1^{3/2})$ together with the prediction from the eddy diffusivity model $\Pi(z) = [1 - (z/z1)^2]^3$ (black, dotted line).

From these fits one obtains a precise determination of $h(t) = 2z_1(t)$, which is plotted in Fig. 2 as a function of time. The compensated plots of $h(t)$ in the inset of Fig. 2 show that in the late stage the mixing layer width grows according to the subdiffusive model $t^{2/5}$. In order to evaluate the accuracy of the numerical simulations, in the inset we show that the compensation with a standard diffusive process, i.e., $h(t) \sim t^{1/2}$, is ruled out.

As the mean temperature profile, shown in Fig. 4, is approximately linear, a simple estimation for the temperature gradient is $\partial_z \overline{T} \simeq \theta_0/h$.

From this expression one obtains for the typical velocity fluctuation in the mixing layer $u_{\text{rms}}^2 \simeq \beta g \theta_0 L_x^2/h$ and, therefore, for the total energy $E \sim u_{\text{rms}}^2 h \sim$ const. in agreement with Fig. 3. The same approximation allows to obtain an estimate for the mean eddy diffusivity as $K \simeq L_x^{8/5} (\beta g \theta_0)^{2/5} t^{-1/5}$, which is consistent with the subdiffusive behavior.

At first glance, the emergence of a subdiffusive behavior may seem counterintuitive because advection adds to the molecular diffusion and greatly enhances the heat transfer. The mechanism which originates this behavior can be qualitatively explained by the following reasoning. The mixing layer grows because of the turbulent motion, but at the same time its growth reduces the effective buoyancy force which sustains the turbulent flow. The result of this negative feedback is that the eddy diffusivity decreases in time, thus leading to the subdiffusive behavior.

It is worthwhile to notice that this regime is expected to last as long as the eddy diffusivity overwhelms the molecular diffusion. A dimensional estimate of the time t_* at which the eddy diffusivity becomes of the same order as the molecular diffusion gives $t_* \simeq (\beta g \theta_0)^2 \kappa^{-5} L_x^8$. At later times one recovers the regime of thermal diffusion.

IV. EFFECTS ON THERMAL CONVECTION

The diffusive model (6) can be used to predict the profile of other dynamical quantities in the turbulent mixing layer. In

particular, as the eddy diffusivity $K(z,t)$ in Eq. (5) replaces the thermal flux $\overline{wT}$ in Eq. (4), from Eq. (7) one has the prediction for the thermal flux profile

$$\overline{wT}(z,t) = \frac{\gamma^{5/2}L_x^2\theta_0(\beta g\theta_0)^{1/2}}{16z_1^{3/2}}\left[1 - \left(\frac{z}{z_1}\right)^2\right]^3 \quad (8)$$

without free parameters as γ is determined by the evolution of $h(t)$. In Fig. 4 we show the compensated thermal flux profile $\Pi(z) = 16z_1^{3/2}\overline{wT}/[\gamma^{5/2}L_x^2\theta_0(\beta g\theta_0)^{1/2}]$ obtained by our numerical simulations after averaging over three independent realizations of the flow. The statistics here are more noisy than for $\overline{T}(z)$ because $\overline{wT}(z)$ has no definite sign. Nonetheless, the prediction given by Eq. (8) without adjustable parameters ($\gamma = 1.40$, obtained from the fit in Fig. 2) fits very well the numerical data.

The relation between the thermal flux and the geometrical properties of the temperature profile can be reformulated in terms of dimensionless quantities. The integral over the mixing layer of $\overline{wT}(z)$ gives the Nusselt number defined as $\mathrm{Nu} = \langle wT\rangle/(\kappa\theta_0 L_x^2)$ which represents the ratio of convective to conductive heat transfer. The Nusselt number is a function of the Rayleigh number, the ratio of buoyancy forces to diffusivity here defined as $\mathrm{Ra} = \beta g\theta_0 h^3/(\nu\kappa)$. By integrating Eq. (8) between $-z_1$ and z_1, one obtains the prediction (again without adjustable parameters)

$$\mathrm{Nu} = \frac{2^{3/2}\gamma^{5/2}}{35}\left(\frac{L_x}{h}\right)^2 \mathrm{Pr}^{1/2}\mathrm{Ra}^{1/2}, \quad (9)$$

where $\mathrm{Pr} = \nu/\kappa$. Equation (9) represents the so-called "ultimate state of thermal convection" predicted by Kraichnan a long time ago [13] for turbulent convection at very high Rayleigh numbers when the contribution of thermal and kinetic boundary layers becomes negligible. This ultimate state regime has been observed in numerical simulations of 3D Rayleigh-Taylor turbulence [14] and in simulations and experiments of bulk turbulent convection [22,23]. With respect to the pure 3D case, in the present configuration the ultimate state regime has the additional coefficient $(L_x/h)^2 < 1$, representing the depletion of the transfer of heat due to the geometrical confinement.

Although the dependence on Ra in Eq. (9) is the same as in 3D RT turbulence, as a consequence of the confinement, the temporal behavior of the dimensionless quantities is different as here we obtain dimensionally $\mathrm{Ra} \sim t^{6/5}$ and $\mathrm{Nu} \sim t^{-1/5}$ while in 3D we have [14] $\mathrm{Ra} \sim t^6$ and $\mathrm{Nu} \sim t^3$. Observe that here the Nusselt number is a decreasing function of time (starting from the value reached in the 3D phase) as a consequence of the fact that the effective temperature jump at the integral scale $\mathcal{L}$ decays in time when $h(t) > L_x$ as discussed before. Therefore, from this point of view the situation here is qualitatively different from the three-dimensional RT configuration in spite of the universality of the scaling of Eq. (9) with respect to the dimensionality.

Figure 5 shows the evolution of Nu compensated both with the geometrical factor $(L_x/h)^2$ as a function of Ra and with $\mathrm{Ra}^{1/2}$ to show the dependence on $h(t)$. In both cases prediction (9) fits well the numerical data, which still display large fluctuations even after averaging over different realizations. The reason for these strong fluctuations (which
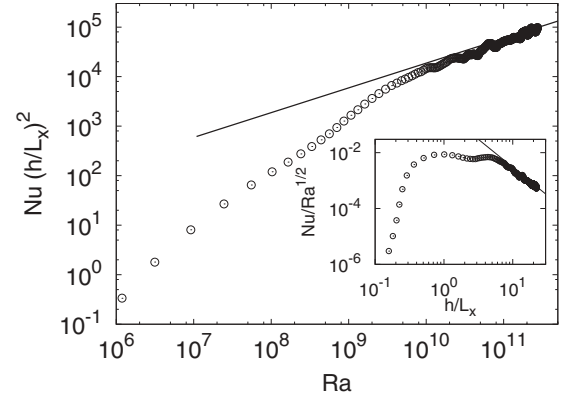

FIG. 5. Nusselt number Nu compensated with the geometrical factor $(h/L_x)^2$ as a function of the Rayleigh number Ra obtained from the average of four independent realizations of the numerical simulation. The line represents the model prediction (9). Inset: Nu compensated with $\mathrm{Ra}^{1/2}$ as a function of the geometrical factor. The line is the dimensional prediction $(h/L_x)^2$.

are not observed in the first stage of 3D dynamics) is due to the fact that at late times, the flow is dominated by a few, large scale (on the order of L_x) thermal plumes. Given these fluctuations, we cannot exclude possible corrections to Eq. (9) as the best fit for the Ra exponent in Eq. (9) gives 0.55 ± 0.05. In the inset of Fig. 5 we observe a plateau for intermediate values of h/L_x; this corresponds to the 3D regime for which an ultimate state scaling $\mathrm{Nu} \sim \mathrm{Ra}^{1/2}$ without geometrical correction is indeed expected.

Small scale statistics in the turbulent flow are represented by the energy spectrum at late times shown in Fig. 6. As a consequence of the geometry of the flow, the spectrum has no support of transverse wave numbers for $k < 8$ where, therefore, the spectrum decays very fast. For larger wave numbers (i.e., scales smaller than L_x, L_y) the energy spectrum displays a short range compatible with Kolmogorov scaling $k^{-5/3}$, followed by a steeper dissipative range. Kinetic energy flux, shown in the inset of Fig. 6, confirms the presence of a direct cascade of kinetic energy. Again, these results support the picture that no turbulent cascade is present at scales
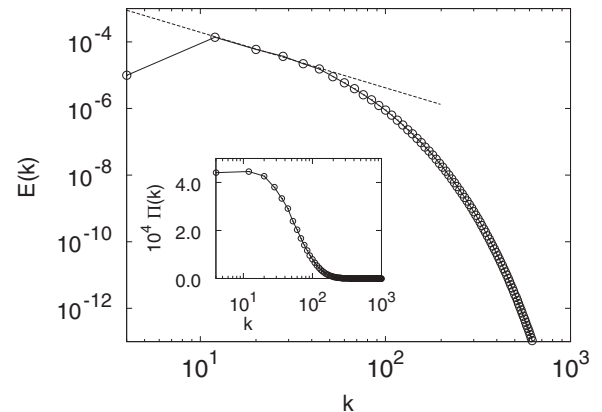

FIG. 6. Kinetic energy spectrum at the final time of the simulation. Wave number $k = 8$ corresponds to the confinement scale L_x. The dotted line represents the Kolmogorov scaling $k^{-5/3}$. Inset: Kinetic energy flux in the wave-number space.

larger than L_x at which an eddy diffusivity model is therefore appropriate.

Because the local effective temperature difference $\theta_{\mathcal{L}}$ which sustains the turbulent flow decreases as the the mixing layer grows, the Reynolds number, defined as $\mathrm{Re} = u_{\mathrm{rms}} L_x / \nu$, decreases as $\mathrm{Re} \sim t^{-1/5}$. The decay of turbulence is accompanied by the growth of the Kolmogorov scale $\eta = (\nu^3/\varepsilon)^{1/4} \sim t^{3/20}$. At late times when the Kolmogorov scale has grown up to the confining scale L_x, the turbulent motion eventually terminates, and the turbulent-subdiffusive regime gives way to a viscous-diffusive regime.

V. CONCLUSIONS

In conclusion, on the basis of high-resolution direct numerical simulations of the Boussinesq equation, we have shown that confinement can induce dramatic changes in the evolution of the turbulent mixing layer in Rayleigh-Taylor convection. In particular we have found that when the width of the mixing layer becomes larger than the scale of lateral confinement, the growth of the mixing layer changes from accelerated to subdiffusive. Interestingly, this phenomenon has been observed also in experiments where boundary conditions on the side walls which confine the flow are completely different from the idealized periodic boundary conditions of our simulations. This seems to suggest that the effects of confinement in turbulent convection may be actually independent of the details of the confining mechanism itself. Further studies may shed new insight on this almost paradoxical conjecture.

[1] D. G. Levitt, Phys. Rev. A **8**, 3050 (1973).

[2] J. Bouchaud and A. Georges, Phys. Rep. **195**, 127 (1990).

[3] D. H. Sharp, Phys. D (Amsterdam, Neth.) **12**, 3 (1984).

[4] D. M. Schultz, K. M. Kanak, J. M. Straka, R. J. Trapp, B. A. Gordon, D. S. Zrnic, G. H. Bryan, A. J. Durant, T. J. Garrett, P. M. Klein, and D. K. Lilly, J. Atmos. Sci. **63**, 2409 (2006).

[5] W. Cabot and A. Cook, Nat. Phys. **2**, 562 (2006).

[6] S. Fujioka, A. Sunahara, K. Nishihara, N. Ohnishi, T. Johzaki, H. Shiraga, K. Shigemori, M. Nakai, T. Ikegawa, M. Murakami, K. Nagai, T. Norimatsu, H. Azechi, and T. Yamanaka, Phys. Rev. Lett. **92**, 195001 (2004).

[7] M. Chertkov, Phys. Rev. Lett. **91**, 115001 (2003).

[8] W. Cabot, Phys. Fluids **18**, 045101 (2006).

[9] S. Dalziel, P. Linden, and D. Youngs, J. Fluid Mech. **399**, 1 (1999).

[10] N. Vladimirova and M. Chertkov, Phys. Fluids **21**, 015102 (2009).

[11] G. Boffetta, A. Mazzino, S. Musacchio, and L. Vozella, Phys. Rev. E **79**, 065301(R) (2009).

[12] T. Matsumoto, Phys. Rev. E **79**, 055301(R) (2009).

[13] R. Kraichnan, Phys. Fluids **5**, 1374 (1962).

[14] G. Boffetta, F. De Lillo, and S. Musacchio, Phys. Rev. Lett. **104**, 034505 (2010).

[15] G. Boffetta, A. Mazzino, S. Musacchio, and L. Vozella, Phys. Fluids **22**, 035109 (2010).

[16] J. Klafter and I. Sokolov, *First Steps in Random Walks: From Tools to Applications* (Oxford University Press, Oxford, UK, 2011).

[17] N. Inogamov, A. Oparin, A. Dem'yanov, L. Dembitskii, and V. Khokhlov, J. Exp. Theor. Phys. **92**, 715 (2001).

[18] S. Dalziel, M. Patterson, C. Caulfield, and I. Coomaraswamy, Phys. Fluids **20**, 065106 (2008).

[19] R. E. Pattle, Q. J. Mech. Appl. Math. **12**, 407 (1959).

[20] M. Baird, K. Aravamudan, N. Rao, J. Chadam, and A. Peirce, AIChE J. **38**, 1825 (1992).

[21] A. Lawrie and S. Dalziel, Phys. Fluids **23**, 085109 (2011).

[22] D. Lohse and F. Toschi, Phys. Rev. Lett. **90**, 034502 (2003).

[23] M. Gibert, H. Pabiou, F. Chillà, and B. Castaing, Phys. Rev. Lett. **96**, 084501 (2006).